



Enhanced retention of hydrophobic pesticides in subsurface soils using organic amendments

Marijana Kragulj Isakovski^a, Irina Jevrosimov^a, Dragana Tamindžija^a, Tamara Apostolović^a, Heike Knicker^b, José María de la Rosa^c, Srđan Rončević^a, Snežana Maletić^{a,*}

^a University of Novi Sad, Faculty of Sciences, Department of Chemistry, Biochemistry and Environmental protection, Trg Dositeja Obradovića 3, 21000 Novi Sad, Republic of Serbia

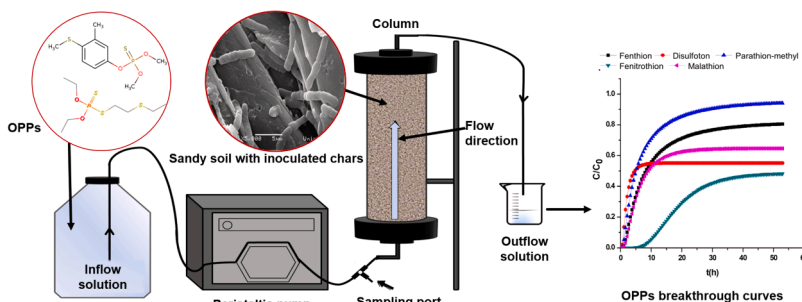
^b Instituto de la Grasa, Consejo Superior de Investigaciones Científicas IG-CSIC, Utrera Rd, Km. 1, 41013 Seville, Spain

^c Instituto de Recursos Naturales y Agrobiología de Sevilla, Consejo Superior de Investigaciones Científicas, IRNAS-CSIC, Reina Mercedes Av., 10, 41012 Seville, Spain

HIGHLIGHTS

- Hydrochar and biochar enhance the retardation of pesticides in sandy alluvial soil.
- Aryl-C makes up approximately 80 % of the total carbon content in the biochars.
- The addition of *Bacillus megaterium* BD5 increases microbial abundance and activity.
- Proteobacteria and Firmicutes are dominant phyla in column soil.

GRAPHICAL ABSTRACT



ARTICLE INFO

Keywords:

Organophosphorus pesticides
Inoculated chars
Retardation
Biosorption
Biodegradation

ABSTRACT

The rapid global population growth since the early 2000s has significantly increased the demand for agricultural products, leading to widespread pesticide use, particularly organophosphorus pesticides (OPPs). This extensive application poses severe environmental risks by contaminating air, soil, and water resources. To protect groundwater quality, it is crucial to understand the transport and fate of these pesticides in soil and sediment. This study investigates the effects of hydrochars and biochars derived from sugar beet shreds (SBS) and *Miscanthus×giganteus* (MIS) on the retardation and biodegradation of OPPs in alluvial Danube sandy soil. The research is novel in its approach, isolating native OPP-degrading bacteria from natural alluvial sandy soil, inoculating them onto chars, and reapplying these bioaugmented chars to the same soil to enhance biodegradation and reduce pesticide leaching. The amendment of chars with immobilized *Bacillus megaterium* BD5 significantly increased bacterial abundance and activity. Metabarcoding of the 16S rRNA gene revealed a dominance of Proteobacteria (48.0–84.8 %) and Firmicutes (8.3–35.6 %). Transport modeling showed retardation coefficients (R_d) for OPPs ranging from 10 to 350, with biodegradation rates varying between 0.05 % and 75 %, indicating a positive correlation between retardation and biodegradation. The detection of biodegradation byproducts, including derivatives of phosphin, pyridine, and pyrazole, in the column leachate confirmed that biodegradation had occurred. Additionally, principal component analysis (PCA) revealed positive correlations

* Corresponding author.

E-mail address: snezana.maletic@dh.uns.ac.rs (S. Maletić).

<https://doi.org/10.1016/j.jhazmat.2024.135738>

Received 19 June 2024; Received in revised form 12 August 2024; Accepted 2 September 2024

Available online 6 September 2024

0304-3894/© 2024 The Authors. Published by Elsevier B.V. This is an open access article under the CC BY license (<http://creativecommons.org/licenses/by/4.0/>).

among retardation, biodegradation, specific surface area (SSA), aldehyde/ketone groups, and bacterial count. These findings demonstrate the potential of biochar and hydrochar amendments to enhance OPP immobilization in contaminated soils, thereby reducing their leaching into groundwater. This study offers a comprehensive approach to the remediation of pesticide-contaminated soils, advancing both our fundamental understanding and the practical applications of environmental remediation techniques.

1. Introduction

The rapid expansion of the global population since the early 2000s has increased the demand for agricultural produce, resulting in widespread usage of pesticides to ensure high crop yields and quality [1]. Annually, more than 20,000 tons of chemical pesticides are applied worldwide, with significant proportions used in the United States and Europe [2]. While pesticides play a crucial role in boosting agricultural productivity, their extensive application poses environmental risks, including contamination of air, soil, groundwater, and surface water. Various types of pesticides are utilized, such as organophosphorus pesticides (OPPs), known for their efficacy and relatively short environmental persistence compared to organochlorine pesticides (OCPs). Despite being considered as a safer alternative, OPPs still contribute to environmental pollution due to their widespread use in farming and industrial activities [3]. Studies suggest that with rising temperatures, pesticide use is expected to increase further, exacerbating ecological concerns [3,4].

Understanding the transport of these pesticides in soil and sediment is crucial as it directly impacts the quality of groundwater, a vital source of drinking water. This transport is primarily governed by sorption and biodegradation processes, which determine the fate and behavior of pollutants in the soil/sediment environment. Thus, investigating these processes and mechanisms are essential for assessing the risk of hazardous substances contaminating drinking water sources [5–8].

To prevent the spread of pollutants through the subsurface, various approaches can be employed [9]. Regarding soil remediation, carbon-rich materials such as biochar and hydrochar offer several benefits, such as carbon sequestration, improved soil fertility, and contaminant immobilization [10,11]. Combining contaminant-degrading microbe inoculation with hydro- and biochars amendment can enhance the biological degradation of pesticides, which offers a promising method for soil remediation [12]. This process entails immobilizing pollutants at and within the biochar allowing their degradation by microbes that are inoculated onto the chars. The adsorption of the organic contaminants helps further preventing their leaching into groundwater [13,14].

Numerous studies have explored the environmental uses of biochar for soil and water remediation and carbon sequestration. For example, Kookana et al. [15] demonstrated biochar's effectiveness in reducing the bioavailability of organic contaminants in soil, while Novak et al. [16] highlighted its role in improving soil fertility and water retention. Bolan et al. [17,18] further investigated biochar's capacity for heavy metal immobilization, emphasizing its multifunctionality in soil amendment. In addition to its role in soil amendment, char has shown promise as a carrier for microbial inoculants aimed at enhancing pollutant degradation. Research by Ajeng et al. [19], Wu et al. [20], Bolan et al. [18], Mahmood Al-Nuaimy et al. [21], and Kamalesh et al. [22] has focused on techniques for immobilizing microorganisms onto chars, categorized into physical and chemical methods [23]. These studies have primarily examined strains originating from contaminated and agricultural soils influenced by organophosphorus pesticides (OPPs) (Liang et al., 2019; Kumar, 2018; [24]; Varyani et al., 2019).

Despite extensive research on biochar and its various applications, a significant gap remains in the literature regarding the isolation and application of OPPs-degrading bacteria from natural alluvial sandy soil. Since the fate of OPPs in this area is less explored, particularly in sensitive regions like bank filtration zones, this study addresses that gap by introducing an innovative approach: for the first time, native strains of

OPPs-degrading bacteria isolated from alluvial sandy soil [7] were used to inoculate biochar and hydrochar. These colonized chars were then reintroduced into the same sandy soil to prevent pesticide leaching and enhance biodegradation. The novelty lies in reintroducing an autochthonous soil strain, already adapted to the local conditions, into its original environment in greater numbers—a strategy not previously explored in the context of riverbank sandy alluvial soils.

The main objective of this study was to determine whether biochars and hydrochars, inoculated with native bacterial strains, could prevent pesticide leaching to groundwater and effectively remediate the soil. To achieve this, biochars and hydrochars derived from two different raw biomasses were inoculated with the native microbial strain and mixed with the original alluvial soil. These mixtures were then packed into stainless steel columns to investigate the transport and potential biodegradation of OPPs.

To confirm and explore the types of interactions involved in this process, all chars were characterized by solid-state Nuclear Magnetic Resonance (NMR) and Thermogravimetric Analysis (TGA). Additionally, Principal Component Analysis (PCA) was conducted to understand the complex interactions between physical, chemical, and microbiological factors and their impact on OPPs behavior. This comprehensive analysis is crucial for advancing knowledge in soil remediation and for scaling up experimental approaches beyond the laboratory scale.

This research not only provides a unique and extensive overview of over 40 observations—spanning physical, chemical, and microbiological factors—but also represents a significant advancement in understanding the complex interactions affecting OPPs in soil. By focusing on native bacterial strains adapted to local conditions, this study offers a novel approach to enhancing biodegradation and preventing pesticide leaching, creating opportunities for future large-scale applications.

2. Materials and methods

2.1. Sample material

Miscanthus × giganteus (MIS) and sugar beet shreds (*Beta vulgaris*, SBS) were utilized as biomass for hydrothermal carbonization (HTC) and pyrolysis. The selection of these feedstocks was based on their distinct chemical compositions, which influence the physicochemical characteristics of the resulting chars. Both materials are rich in cellulose, hemicellulose, and lignin but differ in their relative concentrations: beet shreds contain approximately 30% cellulose and hemicellulose, while miscanthus has about 41.2 % [25,26]. These differing proportions impact the behavior of the biomass during HTC and pyrolysis, with cellulose and hemicellulose producing volatile organic compounds at elevated temperatures [27]. *Miscanthus*, with its higher content of these components, is expected to exhibit different changes in surface area and carbon content compared to beet shreds. Understanding these differences is crucial for tailoring the physicochemical properties of the chars for various applications such as water treatment, soil amendment, and catalyst preparation.

HTC was carried out in a laboratory autoclave (Carl Roth, Model II) under high pressure, with a biomass-to-ultrapure water ratio of 1:15. The suspensions were heated to 180, 200, and 220 °C and agitated at 150 rpm. The resulting hydrochars from MIS and SBS were denoted as HTC_M_180; HTC_M_200; HTC_M_220; HTC_S_180; HTC_S_200, and HTC_S_220. A more detailed procedure of hydrochars production on selected temperatures is given in our previous paper [28] and by other

authors [29] and [30]. For biochar production, the biomass underwent slow pyrolysis at 400 °C in a Model Nabertherm S27. The resulting biochars from *Miscanthus* and sugar beet shreds were designated as B_M and B_S, respectively. The selected pyrolysis temperature range reflects the chemical composition of the feedstocks used. Specifically, the investigated feedstocks (SBS and MIS) are predominantly composed of cellulose and hemicelluloses. As a result, lower and more cost-effective pyrolysis temperatures (below 500 °C) are suitable [25,26]. This temperature range ensures efficient conversion of the biomass into biochar with abundant active binding sites and oxygen functional groups, which enhances adsorption efficiency. Additionally, the feasibility of producing biochar at an attractive price point for investors is more accepted in the regional agricultural market. Further details on the process parameters can be found in our previous publication Kragulj Isakovski et al. [7], but the basic physical (specific surface area, average pore diameter, and pore volume) and chemical (elemental analysis) characteristics of biochar and hydrochars are provided in the [Supplementary material, Table 1](#).

A sandy soil was collected from the Danube River at the drinking water source "Petrovaradinskaada" near Novi Sad (45.261437, 19.866364) following sampling methods ISO 10381-2:2002 and ISO 18512:2007. The organic matter (OM) content was assessed using SRPS EN 12879:2007, while total organic carbon (TOC) was determined with a TOC analyzer (liquiTOCII, Elementar, Germany) following ISO 10694:1995. Our previous paper Kragulj Isakovski et al. [7] provides a detailed description of the methods used and a full characterization of the soil.

2.2. Characterization of the soil and organic soil amendments (OSA)

The solid-state ¹³C NMR spectra of the soil and the hydro and biochar were obtained with a Bruker (Rheinstetten, Germany) Avance III HD 400 MHz wide bore spectrometer, using a triple resonance broadband probe and zirconium rotors of 4 mm OD with KEL-F-caps and applying the variable amplitude cross polarization (CP) technique with a contact time of 1 ms and a magic-angle spinning (MAS) speed of 14 kHz. The spectra of the chars we obtained after acquiring between 4000 and 10 000 scans with a pulse delay was 1 ms. The chemical shift was referenced to the TMS scale and adjusted using the carboxyl C of glycine (176.04 ppm). The spectrum of the soil was obtained after demineralization with 10% hydrofluoric acid according to [31].

For quantification, solid-state ¹³C NMR spectra of soils were divided into four to six chemical shift regions (Knicker 2011c). The range from 220 to 160 ppm is associated with carbonyl/carboxyl C. Between 160 and 110 ppm, sp²C resonances (aryl C or olefin C) are observed. This segment can be further divided into two parts: the O-aryl or phenol C region (160–140 ppm), which includes signals from aryl C or olefins C substituted by O, N, or C, and the aryl C region (140 to 110 ppm), mainly contributed by unsubstituted C. However, here one has to bear in mind that in some aromatic C are also contributing to the region 110 to 90 ppm which overlaps with the signals of anomeric C in carbohydrates. Therefore, in the samples of the charred residues this region was assigned to aromatic C whereas in the spectrum of the soil this region was attributed to O-alkyl C. The core O-alkyl C region ranges from (90 to 60 ppm) and includes signals from carbohydrates, alcohols, and ethers. Signals of N-alkyl C as they occur in amino acids or amino sugars resonate between 60 and 45 ppm, the region which also shows signal of methoxyl C. Resonances between 45 and 0 ppm are attributed to alkyl C in fatty acids, amino acids, or paraffinic structures). Owing to insufficient averaging of the chemical shift anisotropy of aromatic C at a spinning speed of 14 kHz, spinning side bands of their main signal were created at a frequency distance of the spinning speed at both sides of the central signal. They were considered by adding their intensities to that of the parent signal as described in [32].

TGA and its derivative (DTGA) were conducted using the Discovery SDT 650 - Simultaneous TG-DSC device (TA Instruments). In this

process, 5 mg of each sample was placed in an open alumina crucible, which was previously weighed, and subjected to a nitrogen atmosphere with a flow rate of 50 mL/min, which was reduced to 10 mL/min within the microfurnace. The samples were then heated and scanned at a rate of 20 K/min, ranging from 50 °C to 850 °C. The total loss on ignition (TG_{tot}, %) was calculated by integrating the TG curve (expressed in Wg-1) from 50 °C to 850 °C. The TG curve was divided into five distinct sections, each corresponding to different thermal oxidation resistance levels [33]: (i) 50–105 °C, (ii) 105–200 °C, (iii) 200–400 °C, (iv) 400–600 °C, and (v) 600–850 °C. These sections yielded partial weights labeled W1 through W5 corresponding with the relative amounts of moisture, very labile, labile, intermediate, and recalcitrant organic matter+ minerals fractions, respectively. Data on TG, DTGA curves, and mass loss were collected and analyzed using TRIOS software (T.A. Instruments).

2.3. Bacterial biofilm formation on adsorbent

Before commencing the column experiments, it was imperative to inoculate biochar and hydrocharsamples with the BD5 strain, creating an inoculated adsorbent for subsequent utilization in all column and batch experiments. The biochars colonized by BD5 were meticulously examined using scanning electron microscopy (SEM). A procedure was initiated by inoculating a tube containing 3 mL of LB broth with the BD5 strain to achieve an initial optical density (OD₆₀₀) of 0.1, followed by the addition of 50 mg of either biochar or hydrochar. The mixture was then incubated for 24 h at 26 °C and 150 rpm to facilitate the immobilization of vegetative cells on the materials. Post-incubation, 1 mL of the mixture was thrice washed with saline solution to detach unbound cells. The resulting pellets were fixed in 200 µL of 2.5% glutaraldehyde solution for 30 min at ambient temperature and subsequently rinsed thrice with phosphate buffer solution. The supernatant was discarded post-centrifugation at 500 g for 5 min, and the pellet was subjected to SEM analysis using a Jeol JSM-6460LV microscope (Tokyo, Japan). Additionally, a pure culture of BD5 was prepared for SEM analysis by pelleting 1 mL of an overnight LB broth culture and employing the afore mentioned fixation protocol. The isolation and identification methodologies for the BD5 strain have been comprehensively documented in our previous work, Kragulj Isakovski et al. [7]. Strain *B. megaterium* BD5 was successfully immobilized on all 8 materials in the form of vegetative cells. This was confirmed by scanning electron microscopy ([Supplementary material, Fig. 5](#)). Cells were detected on the surfaces of all materials even after multiple washing procedures, indicating they are firmly attached to the materials.

2.4. Column experiment

Transport experiments were conducted in stainless-steel columns (4 cm diameter, 20 cm length) filled with soil amended with various chars previously inoculated with a biofilm of *Bacillus megaterium* BD5.

The biofilm was prepared by inoculating 12 mL of LB medium to a starting OD₆₀₀ of 0.1 and adding 1.75 g of materials. The mixture was then incubated at 26 °C and 150 rpm for 24 h and, washed twice with saline. The resulting pellet containing materials with bound cells was then resuspended in 12 mL of saline. One milliliter of this suspension was used for microbiological analyses, while the remaining 11 mL (containing 1.65 g of material) was mixed with approximately 320 g of soil resulting in 0.5% loading w:w.

In the setup, dry amended sandy soil was added from the top, and a background solution of 0.01 M CaCl₂ was introduced from the bottom using a peristaltic pump for uniform packing. To assess the impact of biochar and hydrochars on pesticide transport, 0.5% of these adsorbents was added. Before introducing thiourea as a tracer, DOC levels and UV absorbance at 254 nm [7] were consistently below 0.5 mg/L and 0.01, respectively, indicating minimal presence of organic matter ([Table 3 in Supplementary materials](#)). These stable measurements suggest that the

char used in the experiment is highly stable and does not release significant amounts of dissolved organic matter. Following this, we introduced thiourea as a tracer at a concentration of approximately 4 mg/L. Eluates were collected and analyzed using a UV-Vis spectrophotometer ($\lambda = 235$ nm), with analysis ending when the thiourea concentration matched the initial. Pesticide-containing solutions were passed through the column, and eluates were collected for pesticide concentration analysis using gas chromatography with mass spectrometry (GC/MS, Agilent 7890 A/5975 C). Additionally, the experiments were conducted under dark conditions using a stainless-steel column, amber bottles, and aluminum foil to prevent photoactivation. This precaution was necessary because dissolved black carbon, potentially derived from biochar, can absorb solar light and produce reactive species that react with contaminants.

Data processing for the transport model in this study is grounded in the analytical solution of the advection-dispersion equation (ADE), which integrates sorption and biodegradation processes according to a first-order rate law [34]. The model used involves fitting three parameters from each experimental breakthrough curve. The retardation factor (R_d) determines the position of the breakthrough curve on the time axis. In cases of biodegradation, the outlet concentration does not reach the initial concentration, and the level of the resulting concentration plateau is influenced by the degradation rate (λ). The effective dispersivity, α_{eff} , influences the sharpness of the breakthrough curve. The raw data used for software modeling is available as open data sets (<https://doi.org/10.5281/zenodo.11235315>). Principal component analysis (PCA) was conducted using PAST 3.22, including the 22 physicochemical properties of the amended soils and retardation and biodegradation of the OPPs.

2.5. Viable bacterial count and enzymatic activity determination

At the start and end of column experiments bacterial counts, enzymatic activities (catalase, dehydrogenase, and phosphatase) and community level physiological profile (CLPP) of microbial community by use of ECOLOG plates were determined.

Bacterial counts (count of cultivable heterotrophic bacteria) in soil and eluate (data not shown) were determined by a spread plate method on yeast extract agar after incubation at 26 °C for 5–7 days. Enzymatic activities were determined by standard methods and expressed per gram of dry mass. Catalase activity was determined by standard permanganometric method [35–37], while acid and alkaline phosphomonoesterase and dehydrogenase activity were determined by standard spectrophotometric methods [38–40].

ECOLOG community level physiological profiles were determined according to manufacturer instructions (Biolog, U.S.A.). First, soil was diluted 1:10 in sterile saline and 130 μ L of dilution was inoculated into ECOLOG plates. Plates were incubated at 26 °C up to 7 days and absorbance at 590 nm was read daily by microplate spectrophotometer (Multiskan GO, Thermo Fisher Scientific). Results were analysed by PCA (principal component analysis) of corrected transformed average well color development (AWCD) data [41–43] using ClustVis web tool [44].

2.6. Bacterial community analysis by 16S rRNA gene metabarcoding

Samples from the columns were collected at the end of experiment and preserved by freezing in liquid nitrogen and stored at –75 °C until DNA extraction. Total DNA was extracted using DNeasyPowerSoil Pro Kit (Qiagen, Netherlands) according to the manufacturer instructions.

Sequencing was commercially performed at the Institute for Molecular Medicine Finland (FIMM) of the University of Helsinki, Finland by protocol for 2 \times 300 paired-end sequencing on Illumina MiSeq sequencer according to standard manufacturer instruction (Illumina, USA). Earth Microbiome primers for hypervariable V4 region of 16S rRNA gene were used: [45,46].

Sequencing data were analyzed using the Quantitative Insights Into

Microbial Ecology 2 pipeline (QIIME2) [47–49]. Taxonomic classification was done by primer-specific classifier for 515-F (Apprill) - 806-R (Parada) primer pair, trained on SILVA 138 database commonly used for 16S rRNA region [50,51].

3. Results and discussion

3.1. Organic matter characterization of the soil and OSAs

The soil used in this study is characterized as a sandy material with low organic matter and TOC contents of 1.02 % and 0.24 %, respectively. The soil mainly consists of sand particles with diameters of 0.200–0.500 mm (>65 %), followed by fine sand (15.5 %) and clay (<10 %). With a permeability of 4.92·10^{–3} cm/s as expected highly permeable.

TGA thermograms are shown in [Supplementary material, Fig. 1](#). The TGA profiles generated for various materials in this investigation display unique characteristics, reflective of their distinct compositions and structural attributes. The TGA profiles are divided into three distinct groups: soil, hydrochars, and biochars ([Supplementary material, Fig. 2](#)), which underscores the differential thermal degradation behaviors intrinsic to each material type. Notably, hydrochars are characterized by a substantial fraction of labile organic matter, constituting 63 % to 78 % of their total content ([Fig. 1](#)), indicating a predominance of readily decomposable organic constituents. This observation aligns with findings from Vučurović [26], which highlighted the abundance of sugars, such as cellulose, hemicellulose, and reducing sugars, in hydrochars. These sugars are prone to rapid decomposition at relatively low temperatures, contributing to the significant mass reduction observed during the labile organic matter phase.

In contrast, biochars exhibit a lower proportion of labile organic matter (11 %), suggesting enhanced stability and resistance to thermal degradation. The mass loss in biochars, between 26 % and 29 % at the intermediate organic matter phase, indicates a mild degree of condensation. The sequence of thermal stability among the studied adsorbents is as follows: hydrochar < biochar < soil, with this pattern being predominantly dictated by the mineral composition of the sandy soil. The high presence of minerals in the sandy soil enhances its thermal stability by acting as thermal buffers that absorb and distribute heat, thus reducing the rate of organic matter decomposition.

Additionally, the enhanced thermal stability observed by TGA, with the relative amounts of intermediate and recalcitrance phases, appears to be associated with increased aromaticity, as demonstrated by NMR findings, and decreased oxygen content, highlighted by the inverse

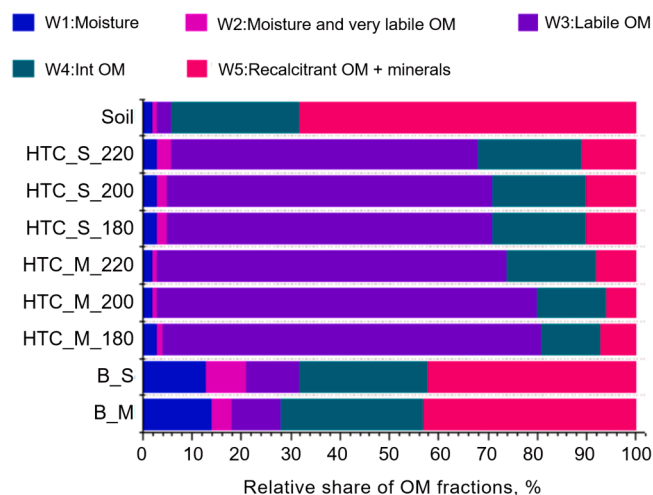


Fig. 1. The relative share of different fractions of organic matter and the total mass loss in the soils, hydrochars and biochars.

relationship with oxygen-containing functional groups. This connection implies that the thermal behavior of organic matter in TGA is predominantly influenced by its aromatic constituents and oxygenated functional groups, as delineated through the characterization with NMR spectroscopy.

The distinct thermal behaviors of hydrochars, biochars, and soil organic matter emphasize the importance of considering the composition and structure of organic matter when investigating thermal characteristics. These findings are corroborated by prior research [52,53], illustrating how organic matter composition influences stability and decomposition, affecting its environmental behavior and interactions.

The NMR spectra of the soil show the typical signals expected for soil organic matter in an advanced stage of humification, which is determined by considerable intensity assignable to carboxyl C (173 ppm) and

a high alkyl C/O-alkyl ratio of 1.4. The latter indicates that carbohydrates such as hemicellulose or cellulose that dominate the C composition of fresh plant litter or roots have been degraded or converted into alkyl C, most likely microbial biomass. The low alkyl C/carbonyl C ratio of 2 suggests that most of the alkyl C occurs in peptide-like structures [54]. The high contribution of aromatic C of 31 % can be derived from the accumulation of lignin residues but may have also some contribution of char residues introduced to the soil during former vegetation fires.

Hydrothermal carbonization leads to a loss of carboxylic C which can explain the 13 C intensity between 185 and 160 ppm in the NMR spectra of the hydrochars [55]. Transformation of the cellulose and hemicellulose of the feedstock into furans is indicated by the clear signal at 147 ppm [56] and the relative high contribution of aromatic C of 20 to 30 % of the total C if compared to vegetal feedstocks. Note that the

Table 1

Transport parameters of selected pesticides through sandy soil and in the presence of inoculated biochar and hydrochars.

Column	Compounds	Water permeability V _w (m/h)	Retardation factor, R _d	Effective dispersivity, α _{eff}	Biodegradation, λ
Soil	Thiourea	1.00	1	0.025	0
	Fenthion	1.00	50	0.03	1
	Disulfoton	1.00	50	0.08	1.2
	Parathion-methyl	1.00	60	0.07	1.3
	Fenitrothion	1.00	55	0.07	1.4
	Malathion	1.00	45	0.03	1.3
Alluvial soil + HTC_M_180	Thiourea	0.760	1	0.03	0
	Fenthion	0.760	100	0.7	10
	Disulfoton	0.760	10	0.1	3.7
	Parathion-methyl	0.760	60	0.5	0
	Fenitrothion	0.760	50	0.15	2.3
	Malathion	0.760	15	0.1	1.7
Alluvial soil + HTC_M_200	Thiourea	0.760	1	0.04	0
	Fenthion	0.760	25	0.09	0.1
	Disulfoton	0.760	18	0.08	0.1
	Parathion-methyl	0.760	15	0.09	0.4
	Fenitrothion	0.760	125	0.35	2.7
	Malathion	0.760	15	0.1	0.05
Alluvial soil + HTC_M_220	Thiourea	1.56	1	0.015	0
	Fenthion	1.56	55	0.1	8.5
	Disulfoton	1.56	50	0.1	12
	Parathion-methyl	1.56	50	0.08	4.5
	Fenitrothion	1.56	60	0.09	3
	Malathion	1.56	55	0.1	2.2
Alluvial soil + B_M	Thiourea	0.828	1	0.002	0
	Fenthion	0.828	60	0.2	1
	Disulfoton	0.828	15	0.1	3.2
	Parathion-methyl	0.828	40	0.2	0.2
	Fenitrothion	0.828	100	0.3	3.3
	Malathion	0.828	40	0.1	2.2
Alluvial soil + HTC_S_180	Thiourea	0.500	1	0.002	0
	Fenthion	0.500	10	0.1	5
	Disulfoton	0.500	20	0.1	2
	Parathion-methyl	0.500	10	0.1	2.5
	Fenitrothion	0.500	10	0.1	2.3
	Malathion	0.500	200	0.9	4.3
Alluvial soil + HTC_S_200	Thiourea	0.600	1	0.02	0
	Fenthion	0.600	30	0.2	1.7
	Disulfoton	0.600	150	0.1	2
	Parathion-methyl	0.600	55	0.2	2.7
	Fenitrothion	0.600	55	0.5	1.7
	Malathion	0.600	55	0.3	1.5
Alluvial soil + HTC_S_220	Thiourea	0.600	1	0.006	0
	Fenthion	0.600	55	0.3	5.5
	Disulfoton	0.600	20	0.1	3
	Parathion-methyl	0.600	50	0.3	2
	Fenitrothion	0.600	45	0.3	2.5
	Malathion	0.600	45	0.3	3
Alluvial soil + B_S	Thiourea	0.980	1	0.03	0
	Fenthion	0.980	35	0.008	6.2
	Disulfoton	0.980	45	0.01	5
	Parathion-methyl	0.980	75	0.1	1.5
	Fenitrothion	0.980	15	0.1	1.7
	Malathion	0.980	350	0.02	75

hydrochars of MIS depict a higher aromatization (relative content of aromatic C), but a lower relative content of alkyl C than the hydrochars of SBS pointing to the impact of the chemical composition of the feed-stock on the nature of the pyrolyzed product.

The high temperatures applied during dry pyrolysis are responsible for a more pronounced change of the chemical structure towards increasing aromaticity. Around 80 % of the total C of the biochars can be attributed to aryl C. The small shoulder at 154 ppm reveals that the presence of phenol C. It was suggested that they are formed during thermally induced condensation of furan structures at pyrolysis temperatures above 400 °C [56]. These aromatic structures are commonly related to their biochemical recalcitrance and made responsible for the longevity of biochar in soils.

Pyrolysis leads to dehydration and condensation which increases the aromaticity. The smaller residues that were cut off from the cellulose strain are lost by volatilization or by their transformation into CO₂. The latter comprise the thermally labile fraction. This fraction is lost both for the NMR but also will not be analyzed by TGA. Thus, the NMR shows the structures that were stable enough to survive pyrolysis. Those structures should also show “stable behavior” in the TGA.

3.2. Column experiment

Column experiments study the effects of addition of specific chars on the transport of OPPs through sandy soil. The breakthrough curves for fenthion, disulfoton, parathion-methyl, fenitrothion, and malathion, along with a tracer (thiourea), are shown in [Supplementary material, Fig. 3](#). Statistical analysis confirms no significant differences between three replicates ($P > 0.05$) based on One-way ANOVA.

The symmetrical breakthrough curve for tracer thiourea confirms that there are no physical nonequilibrium processes within the porous media. Transport parameters (retardation coefficients, R_d) and biodegradation rates (λ) for OPPs through the columns are determined using TransMod software ([Table 1](#)). Retardation coefficients for all OPPs in sandy soil are similar, ranging from 45 to 60, while biodegradation coefficients show even more similarity, ranging from 1.5 to 2. The steepness of the breakthrough curve indicates the extent of nonlinear sorption. Mobility of fenthion through only sandy soil ($\alpha_{eff}=0.03$) exhibits steeper breakthrough curves compared to disulfoton and methyl-

parathion ($\alpha_{eff}=0.7-0.8$), indicating a lower degree of nonlinear sorption for both pesticides. Moreover, incomplete breakthrough curves for all OPPs suggest the presence of biodegradation in the column.

For the column filled only with sandy soil, the retardation coefficients do not correlate with the hydrophobicity of the compounds ($R^2 \sim 0.2$, not shown). This suggests that the retention mechanism of organophosphorus pesticides (OPPs) cannot be solely attributed to hydrophobic interactions between the compounds and the SOM. This discrepancy in sandy soil may be due to the low levels of SOM (TOC content 0.24 %), which contain a higher proportion of O-alkyl functional groups (28 %) as indicated by NMR results ([Fig. 2](#)). These findings are consistent with recent literature that emphasizes the complex nature of sorption processes on SOM and the need to consider additional factors beyond hydrophobic interactions [57]. Apostolović et al. [58] demonstrated through PCA that sorption could be influenced by physical parameters, such as specific surface area (SSA) and clay content. In contrast, the H/C ratio exhibited the lowest loading, indicating a lesser impact on sorption behavior.

Further column studies are being conducted to investigate the influence of different inoculated hydrochars and biochars on overall retention in a sandy column, using the same experimental approach as with the columns packed solely with soil. Since previous results have shown that biodegradation or biosorption occurs in sandy soil columns, the aim is to enhance the biosorption/biodegradation potential of hydrochar and biochar by introducing bacteria capable of degrading organophosphorus pesticides. These bacteria are isolated from sandy soil and colonized onto these materials as confirmed by SEM ([Supplementary material, Fig. 5](#)).

As expected, the addition of hydrochars and biochars increases the retardation of all investigated OPPs compared to the retardation coefficients obtained for the column filled only with sandy soil, mostly by one or two times, except for malathion ([Table 1](#)). Additionally, the obtained R_d values for the tested compounds are not consistent with their hydrophobicity. There are no observed correlations between the R_d values of OPPs and the compounds' hydrophobicity expressed as logK_{OW} (octanol-water coefficient), except for hydrochar from miscanthus at 180 ($R^2=0.792$) (data not shown). These findings directly demonstrate that the incorporation of inoculated carbon-rich materials could substantially enhance retardation throughout the column, likely

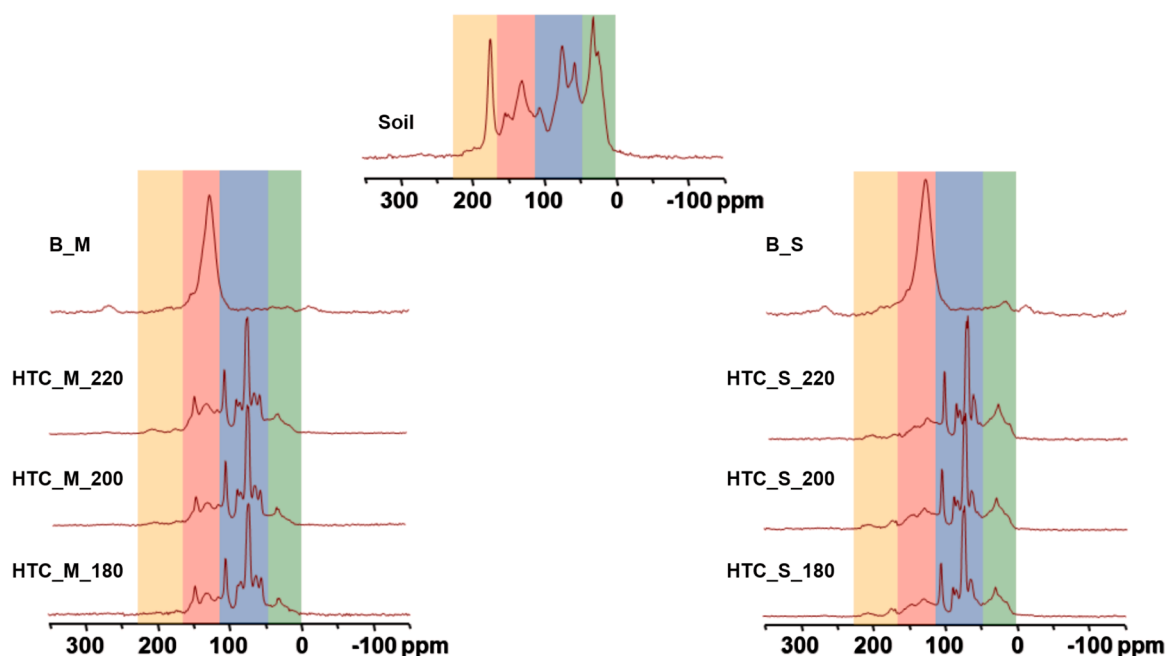


Fig. 2. ¹³C NMR spectra of soil, hydrochars and biochars.

attributable to biosorption.

Comparing the biodegradation coefficients for all the investigated compounds using a first-order rate law, the inclusion of chars boosts the biodegradation of the examined compounds by up to tenfold, except for malathion when biochar from SBS is present. Top of Form.

A positive correlation was found between the retardation and biodegradation coefficients ($R^2 > 0.7$), indicating that the increase in biodegradation was consistent with the retardation of compounds in the column (Fig. 3).

The retention of pesticides on adsorbents inoculated with BD5 suggests that an initial step in biodegradation may involve the attachment of OPPs to biochars and hydrochars, which then facilitates further biodegradation. This mechanism is supported by our previous study [7], which showed that the presence of carbon-rich materials could enhance both the adsorption and biodegradation of OPPs.

The chemical structure of biochars and hydrochars is crucial in their interaction with OPPs. Biochars, characterized by their π -electron-rich regions (about 80 % attributed to aryl C), are particularly effective at forming π - π interactions with OPPs. These π -electrons, present in the aromatic structures of biochars, create electron-rich areas that can attract and stabilize the π -electrons in the aromatic rings of OPPs. This interaction could be described as stacking two flat surfaces together, where the aligned aromatic rings enhance the adsorption of these compounds onto biochar surfaces. Recent studies have corroborated the efficacy of biochars in adsorbing organic pollutants through π - π interactions. For instance, Zhou et al. [59] demonstrated that biochars derived from agricultural residues exhibited strong π - π interactions with polycyclic aromatic hydrocarbons (PAHs), similar to the interaction mechanism observed with OPPs. This supports the idea that the aromatic structure of biochars plays a central role in pollutant adsorption, particularly for compounds with aromatic characteristics.

In contrast, hydrochars exhibit a unique chemical composition with higher proportions of anomeric carbon, O-alkyl groups, methoxyl groups, and N-alkyl carbon (65 % of the identified functional groups as shown by NMR). While these functional groups can promote electron donor-acceptor (EDA) interactions with OPPs, the most significant

mechanism for hydrochars could be hydrogen bonding.

Hydrochars possess hydroxyl ($-\text{OH}$) groups that act as hydrogen donors, interacting with phosphate groups in OPPs, which function as hydrogen acceptors. This hydrogen bonding interaction provides a strong and stable binding between the hydrochar surface and OPPs, analogous to a magnet attracting and holding onto an object. This mechanism enhances the adsorption capacity of hydrochars, making them particularly effective in capturing and retaining these pollutants.

The role of hydrogen bonding is further supported by a study from Du et al. [60], which highlighted the importance of hydrogen bonding in enhancing the adsorption of organophosphorus compounds on chars with high hydroxyl group content. This aligns with our findings that hydrogen bonding is a critical factor for effective adsorption in hydrochars.

However, the presence of anomeric carbon in hydrochars shows a negative correlation with the retardation and biodegradation of OPPs (Fig. 6). This observation suggests that higher levels of anomeric carbon are associated with reduced effectiveness in slowing down the movement and degradation of OPPs. Despite its contribution to EDA interactions, the negative correlation indicates that anomeric carbon may not be as beneficial in terms of retardation and biodegradation compared to the hydrogen bonding mechanism.

Oxygen-containing functional groups in hydrochars play a dual role: they not only enhance adsorption through hydrogen bonding but also facilitate microbial activity, which aids in the breakdown of pollutants. Recent research by Li et al. [61] emphasizes this significance, showing that electrostatic and hydrogen-bonding interactions are the primary mechanisms for adsorbing methylene blue onto hydrochars. This study supports the notion that hydrogen bonding is a key factor in maximizing the environmental performance of hydrochars.

3.3. Bacterial community composition and activity in column experiments

To further assess biodegradation potential within the column, a series of microbiological and biochemical analyses were conducted. At the start and end of experiment bacterial counts, enzymatic activities

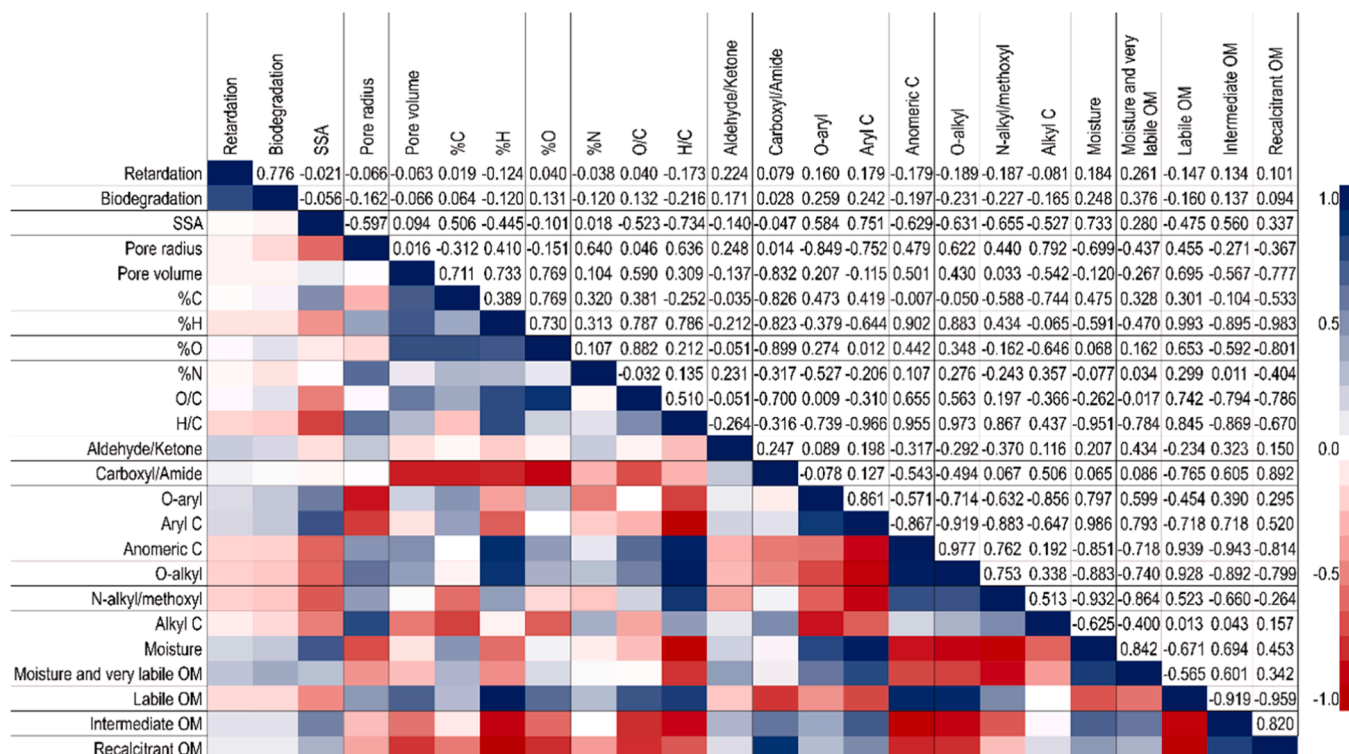


Fig. 3. Relationship between physicochemical characteristics, biodegradation and retardation.

(catalase, dehydrogenase, and phosphatase) and CLPP of microbial community by use of ECOLOG plates were determined. To that, bacterial community composition was determined by 16S rRNA gene metabarcoding.

Cultivable bacterial counts in column mixture at the start of experiment were in 10^5 – 10^6 CFU/g range and have increased approximately ten-fold in all column experiments by the end of the experiment, resulting in final counts ranging from 10^6 to 10^7 CFU/g depending on the column (Supplementary material, Fig. 4). There was no statistically significant difference between SBS and MIS materials nor between hydrochars and biochars (Mann Whitney U test, $p > 0.05$). Slightly higher starting counts were noted for both biochar samples (B_S and B_M), indicating that these materials can incorporate more immobilized cells of BD5 under the same biofilm preparation procedure, compared to other materials. This could be attributed to their higher SSA, smaller pore radius and presence of micropores (Table 1 in Supplementary materials). This all could enable better bacterial colonization and immobilization. To that, biochars have higher C content (elemental analysis) and high aromaticity (around 70 %) which could indicate that more carbon sources are available for microbial utilization. On the other hand, this may also be a disadvantage, since the microorganisms may feed on the biochar rather than on the pollutants. Higher bacteria colonization could also be linked to the biochar's higher content of aryl C-H, O-aryl and carboxyl carbohydrates as determined by NMR (Fig. 2), and higher percentage of intermediate and recalcitrant organic matter as found by thermogravimetric analyses (Fig. 1).

It should be noted that assessing microbial count and activity via measurement of cultivable bacterial counts has some methodological drawbacks. Specifically, cultivable microorganisms make up only a minor fraction of total present microorganisms (less than 1 %), as majority of microorganisms will not be cultivable under the stated laboratory conditions [62]. Thus, other approaches such as 16S rRNA

metabarcoding, metatranscriptomics and metagenomics could offer better insights into microbial community composition and functionality.

Enzyme activity values both at the start and the end of column experiments were very low (Supplementary material Fig. 4). Better insight into the metabolic state of the microbial community in the column experiment was obtained by Ecoplates assay. Community level physiological profiling (CLPP) using Ecoplates revealed that uninoculated control soil exhibited different microbial community activity compared to all other column mixtures which contained hydrochar/biochars and strain BD5 (Fig. 4), as evidenced through PCA analysis of AWCD corrected well absorbance values. No apparent grouping of utilized substrate groups was noted based on PCA. Overall, much lower activity was noted in control soil sample, compared to samples inoculated with materials and BD5 strain. This all indicated that inoculation of soil with materials loaded with biofilm of BD5 strain significantly increased metabolic activity of microbial community, which could result in improvement of biosorbing and biodegrading processes in the columns. No statistically significant difference among different materials was noted.

16S rRNA gene metabarcoding allowed detailed insight into the structure and relative abundance of bacterial community at the end of column experiments (Fig. 5). The most abundant bacterial phyla in all the samples were Proteobacteria (48.0 - 84.8 %) and Firmicutes (8.3 - 35.6 %). Inoculated strain *B. megaterium* BD5 belongs to phylum Firmicutes and probably has contributed to high relative abundance of Firmicutes. Exact detection of *B. megaterium* BD5 could not be accomplished as 16S rRNA gene metabarcoding resolution is insufficient for reliable species level determination. However, the most predominant genus was *Bacillus* with an average relative frequency of 10.2 ± 6.7 % (Table 2 of the Supplementary material). Beside Bacillaceae, other most frequent families were Oxalobacteraceae, Caulobacteraceae and Pseudomonadaceae. These families encompass various members which

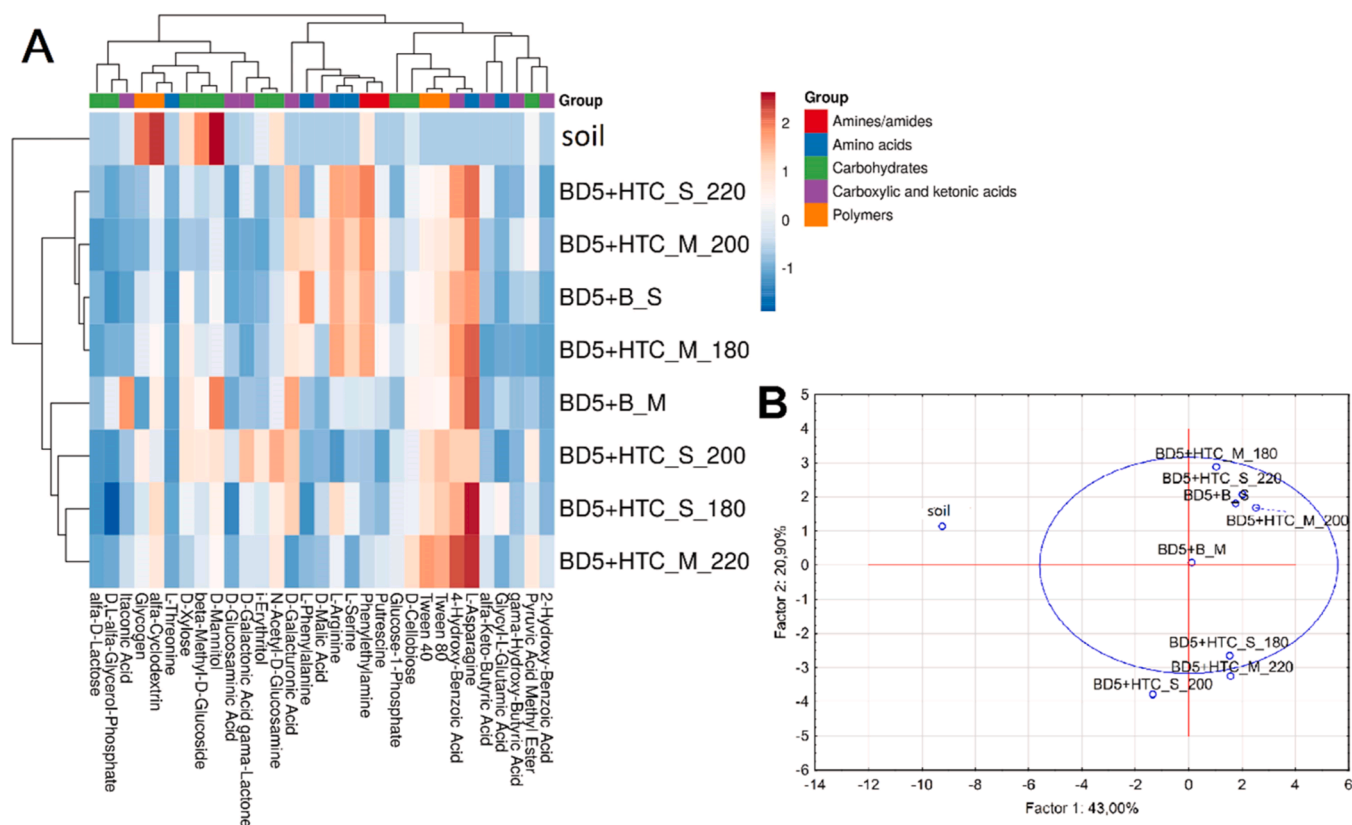


Fig. 4. Community level physiological profiling of column samples at the end of experiment analysed by Ecoplates utilization patterns of 31 carbon sources after 3 days of incubation – principal component analysis.

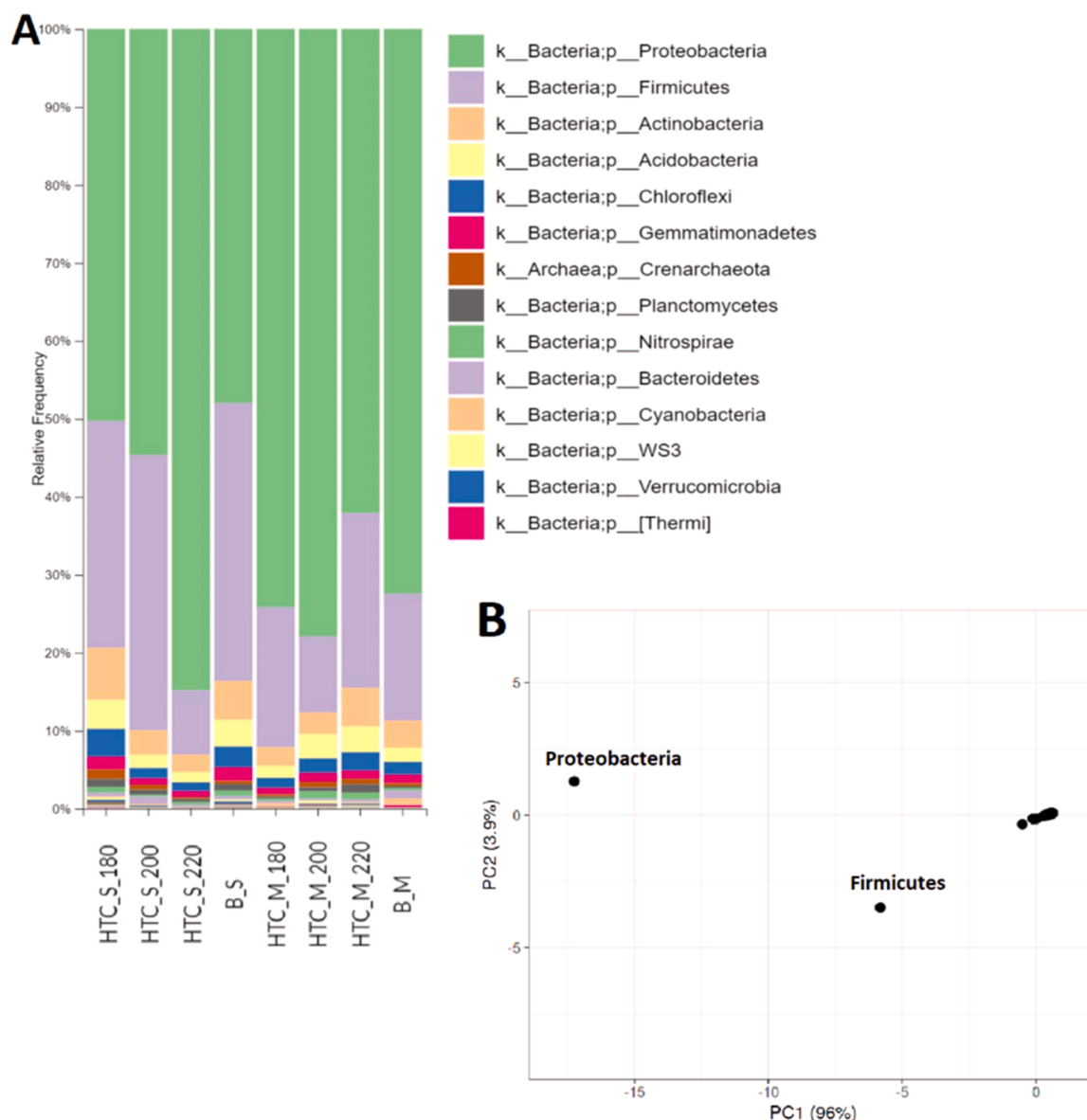


Fig. 5. Bacterial community composition determined by sequence analysis of 16S rRNA gene: A – relative composition on phylum level, B – principal component analysis.

commonly inhabit soil, fresh and marine aquatic environments and have a significant role in nutrient cycling and organic matter decomposition, including pollutants. *Pseudomonas* species are especially well known for their diverse metabolic capabilities and high OPPs biodegradation potential, as they produce enzymes such as phosphotriesterases and organophosphorus hydrolase, which can break down organophosphorus compounds [63]. As with bacterial count, enzyme activity and Ecoplate CLPP results, there was no apparent difference among SBS and MIS materials nor between hydrochars and biochars based on 16S rRNA bacterial community profiling.

Biochar effect on soil microbial communities is complex and multifaceted, with both positive and negative outcomes depending on the specific conditions, such as soil and biochar properties. While biochar generally promotes microbial diversity and activity, careful consideration of biochar properties, application rates, and soil characteristics is essential to maximize its benefits and minimize potential drawbacks. Char amendments in soil can influence microbial community composition particularly in terms of the increased relative abundance of certain bacterial phyla such as Proteobacteria, Actinobacteria, Firmicutes, Cyanobacteria, Bacteroidetes and Acidobacteria (Jenkins et al., 2017;

[64]). These phyla are crucial for various soil functions, including nutrient cycling and organic matter decomposition. However, effects of char addition can vary widely depending on initial soil community composition, soil properties and char properties [65,66]. Our study confirmed similar trends in microbial community shift (dominance of Proteobacteria, Firmicutes, Actinobacteria and Acidobacteria) and specific increase in *Pseudomonas* and *Bacillus* species in amended soil previously reported also by Singh et al. [67]. Accordingly, our 16S barcoding results highlight the fact that bacteria crucial in organic matter decomposition and pollutant biodegradation were prominent members of the column bacterial community.

Although next-generation sequencing and 16S rRNA gene metabarcoding have immensely improved our understanding of microbial communities of various environments, it is important to acknowledge the methodological limitations of 16S rRNA gene metabarcoding [68]. This methodology identifies the microbial taxa present in a sample and their relative abundance but does not accurately assess their viability or metabolic activity. This limitation arises from the fact that DNA from inactive or dead cells can still be detected, potentially leading to an overestimation of the active microbial community. In future studies,

employing methodologies such as metagenomics, metatranscriptomics, metaproteomics, and metametabolomics could provide a more comprehensive understanding of microbial activity and offer deeper insights into the functional dynamics and metabolic networks of the microbial community, including its interactions with physicochemical processes.

Overall, microbial analyses indicate efficient immobilization of bacterial strain *B. megaterium* BD5 on biochar and hydrochar materials made from sugar beet shreds and *Miscanthus* \times *giganteus*. Results show a significant increase of viable bacterial counts and functional activities in amended columns compared to unamended ones. Overall, microbial community composition, abundance and functional activity did not differ between the columns amended with different materials. This indicates that addition of bacterial strain *B. megaterium* BD5 had a major impact on overall microbial characteristics. The bacterial community was dominated by taxa with important roles in nutrient cycling and organic matter decomposition such as Bacillaceae, Oxalobacteraceae, Caulobacteraceae and Pseudomonadaceae, with prevalence of genera *Bacillus* and *Pseudomonas*.

Understanding the metabolic networks and pathways utilized by microbes in biodegradation processes can be significantly enhanced through detailed analysis of experimental columns. These insights are crucial for improving bioremediation strategies. For instance, the biodegradation pathways of investigated organophosphorus pesticides, as illustrated in Fig. 6 of the Supplementary materials, reveal complex reactions involving hydrolysis, oxidation, reduction, hydroxylation, and ring cleavage. The biodegradation of organophosphorus pesticides such as Fenthion, Disulfoton, Parathion-methyl, Fenitrothion, and Malathion typically begins with hydrolysis catalyzed by microbial phosphotriesterases, resulting in the cleavage of P-O or P-S bonds and the release of corresponding thiols or alcohols [63]. Following hydrolysis, oxidative reactions catalyzed by microbial monooxygenases and dioxygenases introduce hydroxyl groups to aromatic rings or alkyl chains, leading to intermediates such as hydroxylated fenthion oxon and p-nitrophenol. The nitro groups in compounds like Parathion-methyl and Fenitrothion are reduced to amino groups by nitroreductases (Boddu et al., 2021). These processes produce degradation

intermediates that further transform into products like 3-(6-Methyl-3-pyridyl)-1,5-di(p-tolyl)-2-pyridine, Diphenyl(m-carboxyphenyl) phosphine, and 5-Butyl-3-methyl-1-(4-nitrophenyl) pyrazole. Specifically, 3-(6-Methyl-3-pyridyl)-1,5-di(p-tolyl)-2-pyridine forms from hydroxylation and ring cleavage of pyridyl intermediates, Diphenyl (m-carboxyphenyl) phosphine arises from oxidative cleavage of organophosphorus compounds (as shown in Fig. 6), and 5-Butyl-3-methyl-1-(4-nitrophenyl) pyrazole results from cyclization of nitrophenyl and alkyl-containing intermediates. These sequential enzymatic reactions highlight comprehensive biodegradation pathways involving oxidation, reduction, hydroxylation, and ring cleavage, leading to the final detected byproducts. This is further supported by the identification of enzymes such as phosphotriesterases and Mes11 NfrA1 and NfrA2 nitroreductases in other strains of *Bacillus megaterium* [69]. Also, genera of bacteria possessing phosphotriesterases (e.g. *Pseudomonas*, *Flavobacterium*) or other gene variants (e.g. *Deinococcus*, *Mycobacterium*, *Geobacillus* and *Thermoaerobacter*) and nitroreductases (e.g. *Pseudomonas*, *Bacillus*, *Stenotrophomonas*) [70,71] have been detected in the columns by the 16S rRNA metabarcoding. Additionally, it is noteworthy that during the time course of the column experiments, the intensity of identified byproduct peaks increased (from approximately 1440 min to 3000 min), indicating a rise in the concentration of these compounds in the column leachates (Fig. 6 in Supplementary materials).

3.4. Overall impact of hydrochar and biochar on OPPs retardation and biodegradation

The PCA biplot analysis (Fig. 6) provides a comprehensive view of the relationships between variables influencing the retardation and biodegradation of organophosphorus pesticides (OPPs) in soil columns. The directions of the vectors (as numbered in the biplot) are crucial for understanding both positive and negative correlations, which are essential for interpreting how various factors contribute to the fate of OPPs in this experimental setup.

Strong positive correlations are observed between retardation, biodegradation, and several key variables, such as the content of

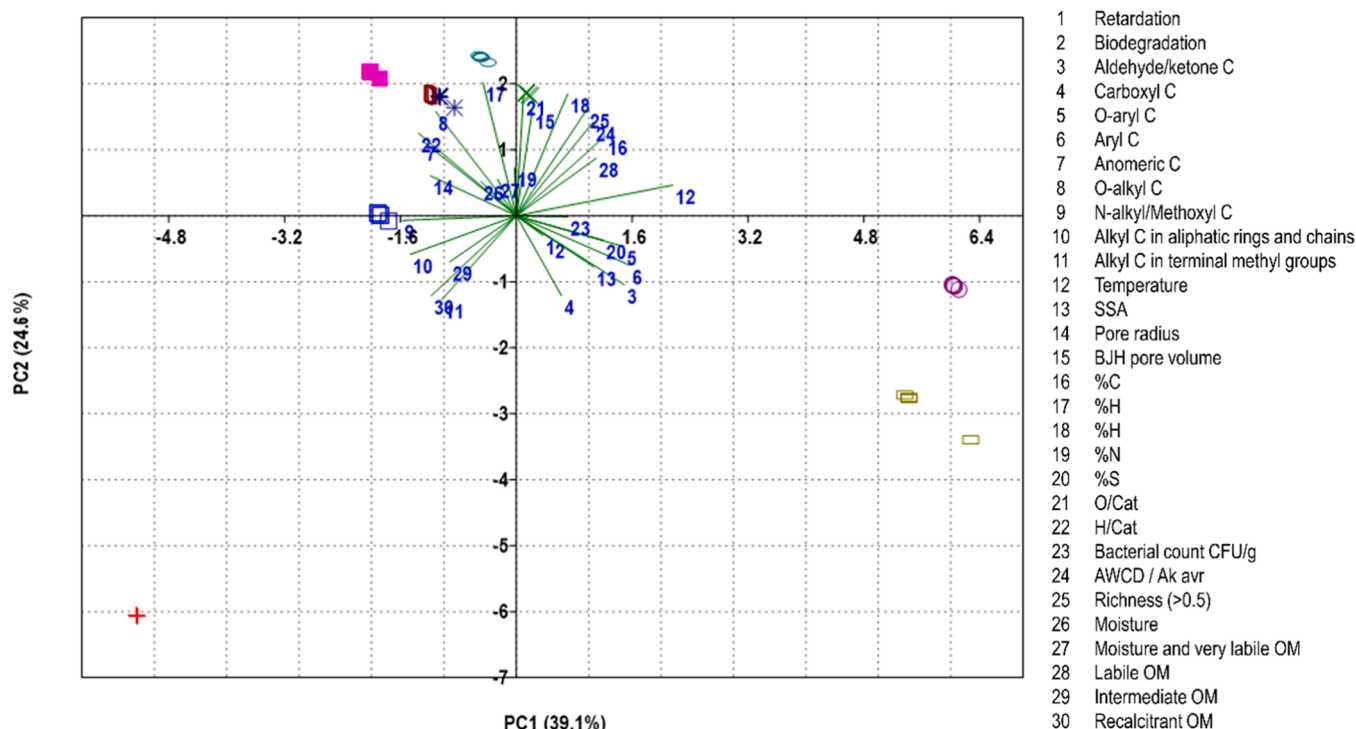


Fig. 6. PCA biplot analysis of physicochemical and microbiological parameters affecting the retardation and biodegradation of organophosphorus pesticides.

aldehyde/ketone groups, SSA and microbiological factor like bacterial count. In the biplot, the vectors representing aldehyde/ketone groups (3), SSA (13), and bacterial count (23) are aligned with those for retardation (1) and biodegradation (2). This alignment suggests that these factors work synergistically to enhance the retention and breakdown of OPPs within the soil matrix. The presence of these functional groups on the char surface creates more reactive sites, which are crucial for adsorbing pollutants and thus delaying their movement through the soil (retardation). This is consistent with our previous observations that oxygen-containing functional groups play a crucial role in enhancing adsorption properties through H-bonding with OPPs. Additionally, these reactive sites also facilitate microbial activity, leading to more effective biodegradation. A higher SSA implies more available surface for interactions between OPPs and chars, further enhancing retardation by trapping OPPs and providing a conducive environment for microbial degradation. This is supported by the positive correlation observed between the retardation and biodegradation coefficients, with an $R^2 > 0.7$ (Fig. 3). Moreover, a higher SSA enhances microbial adhesion, leading to increased microbial counts and activity, and consequently increased biodegradation of OPPs. The alignment of the bacterial count vector with those of retardation and biodegradation emphasizes the critical role of microbial activity in the behavior and fate of OPPs.

Conversely, negative correlations are observed between retardation, biodegradation, and factors such as anomeric carbon (7), the H/C ratio (22), and moisture (26). The vectors for these variables point in directions nearly opposite to those of retardation and biodegradation, indicating inverse relationships. Anomeric carbon, which refers to the carbon atom in a sugar molecule involved in the formation of the glycosidic bond, is often associated with more complex and less stable organic structures. These structures may provide fewer attachment sites for organophosphorus pesticides (OPPs), thereby reducing the char's ability to retain OPPs. Consequently, this leads to increased mobility of OPPs through the soil, as the presence of anomeric carbon appears to diminish the char's effectiveness in retaining these contaminants.

Additionally, a higher H/C ratio implies the presence of less aromatic and more labile carbon structures, which is characteristic of hydrochars, as shown in Fig. 2. This results in decreased retardation and biodegradation efficiency as aromaticity increases, highlighting the significant role of other interactions, such as hydrogen bonding, particularly in the case of hydrochars. The critical importance of hydrogen bonding is further highlighted by the negative correlation observed between anomeric carbon and the retardation and biodegradation of OPPs.

In contrast, biochars, being more aromatic with lower H/C ratios, demonstrate the impact of π - π interactions and possess structural properties that better support microbial activity, thereby enhancing biodegradation. The higher bacterial count observed in biochars may be attributed to their greater SSA, a lower H/C ratio and higher aromaticity—factors that collectively enhance biodegradation.

Based on these observations, it can be concluded that hydrochars are characterized by a lower degree of aromaticity and higher H/C ratios, which suggest the potential for significant interactions such as hydrogen bonding. In contrast, biochars exhibit greater aromaticity and lower H/C ratios, indicating the prominence of π - π interactions. These structural properties of biochars are likely to better support microbial activity and enhance biodegradation processes.

The role of char is critical in both retention and biodegradation processes. The char's specific surface area and functional groups not only absorb OPPs but also create a stable matrix that supports enzymatic reactions involved in biodegradation pathways. The interaction between char and microbial communities enhances the transformation of OPPs into smaller byproducts. The observed increase in the intensity of byproduct peaks over time in the experimental columns suggests that char actively facilitates the continuous biodegradation of OPPs. The combined analysis of the biplot and biodegradation pathways highlights char's dual function as both a physical barrier that retards pollutant movement and a catalyst that promotes microbial degradation. This

comprehensive understanding of char's impact on the retention and degradation of OPPs emphasizes its effectiveness in environmental remediation efforts, underlining the importance of considering these dynamic interactions when applying biochar for pollutant management.

4. Conclusions

This study demonstrates that hydrochars and biochars derived from sugar beet shreds and miscanthus significantly enhance the retardation and biodegradation of organophosphorus pesticides (OPPs) in sandy soil. Using ^{13}C NMR and TGA, we gained valuable insights into the structural and functional properties of these amendments, highlighting the crucial roles of aromatic structures and oxygen-functional groups in stabilizing and facilitating biodegradation processes. The successful immobilization of OPP-degrading bacterial strain onto the chars led to increased microbial abundance and functionality within the soil columns. Additionally, 16S rRNA-based bacterial community profiling identified taxa with significant roles in the biodegradation of organic compounds, including pollutants. These findings advance our understanding of the interactions between organic amendments and pollutants, emphasize the potential of these adsorbents to enhance soil remediation practices and improve pesticide management in agricultural settings.

Environmental implication

For the first time, we have successfully isolated and applied organophosphorus pesticide (OPP)-degrading bacteria from natural alluvial sandy soil. Previous studies have focused on strains from contaminated and agricultural soils. Our approach involved colonizing biochar and hydrochar with these bacteria and reintroducing them into the same sandy soil to prevent pesticide leaching and enhance biodegradation. The novelty of this work lies in using autochthonous strains, already adapted to local conditions, in greater numbers within their native environment. This significant achievement improves our understanding of in situ remediation potential for contaminated soils and sediments.

Funding

Funded by the European Union. GA No. 101059546-TwinSubDyn. Views and opinions expressed are however those of the author(s) only and do not necessarily reflect those of the European Union or European Research Executive Agency (REA). Neither the European Union nor the granting authority can be held responsible for them.

CRediT authorship contribution statement

Dragana Tamindžija: Writing – original draft, Methodology, Investigation, Conceptualization. **Tamara Apostolović:** Writing – original draft, Software, Methodology, Investigation. **Heike Knicker:** Writing – original draft, Methodology, Data curation, Conceptualization. **José María de la Rosa:** Writing – original draft, Methodology, Conceptualization. **Srdan Rončević:** Writing – review & editing, Data curation, Conceptualization. **Snežana Maletić:** Writing – review & editing, Supervision, Resources, Methodology, Funding acquisition. **Marijana Kragulj Isakovski:** Writing – original draft, Methodology, Investigation, Conceptualization. **Irina Jevrosimov:** Writing – original draft, Software, Methodology, Formal analysis, Conceptualization.

Declaration of Competing Interest

The authors would like to declare that they have no conflicts of interest associated with this paper.

Data Availability

Data will be made available on request. The datasets used or analyzed during the current study are available from the corresponding author upon reasonable request. Additionally, the datasets are hosted in the Zenodo repository at <https://doi.org/10.5281/zenodo.11235315>

Appendix A. Supporting information

Supplementary data associated with this article can be found in the online version at [doi:10.1016/j.jhazmat.2024.135738](https://doi.org/10.1016/j.jhazmat.2024.135738).

References

- Alrefaie, S.H., Aljohani, M., Alkhamis, K., Shaaban, F., Desouky, M.G.E., El-Bindary, A.A., et al., 2023. Adsorption and effective removal of organophosphorus pesticides from aqueous solution via novel metal-organic framework: adsorption isotherms, kinetics, and optimization via Box-Behnken design. *J Mol Liq* 384, 122206. <https://doi.org/10.1016/j.molliq.2023.122206>.
- Rani, L., Thapa, K., Kanojia, N., Sharma, N., Singh, S., Grewal, A.S., et al., 2020. An extensive review on the consequences of chemical pesticides on human health and environment. *J Clean Prod* 283, 124657. <https://doi.org/10.1016/j.jclepro.2020.124657>.
- Montuori, P., De Rosa, E., Di Duca, F., De Simone, B., Scippa, S., Russo, I., et al., 2022. Occurrence, distribution, and risk assessment of organophosphorus pesticides in the aquatic environment of the Sele River Estuary, Southern Italy. *Toxics* 10, 377. <https://doi.org/10.3390/toxics10070377>.
- Diab, K.E., Salama, E., Hassan, H.S., El-Moneim, A.A., Elkady, M.F., 2021. Bio-zirconium metal-organic framework regenerable bio-beads for the effective removal of organophosphates from polluted water. *Polymers* 13, 3869. <https://doi.org/10.3390/polym13223869>.
- Bertelkamp, C., Reungoat, J., Cornelissen, E.R., Singhal, N., Reynisson, J., Cabo, A., et al., 2014. Sorption and biodegradation of organic micropollutants during river bank filtration: a laboratory column study. *Water Res* 52, 231–241. <https://doi.org/10.1016/j.watres.2013.10.068>.
- Jevrosimov, I., Kragulj Isakovski, M., Apostolović, T., Tamindžija, D., Rončević, S., Sigmund, G., et al., 2023. Microbially inoculated chars strongly reduce the mobility of alachlor and pentachlorobenzene in an alluvial sediment. *Integr Environ Assess Manag* 19 (4), 933–942. <https://doi.org/10.1002/ieam.4691>.
- Kragulj Isakovski, M., Maletić, S., Tamindžija, D., Apostolović, T., Petrović, J., Trčković, J., et al., 2020. Impact of hydrochar and biochar amendments on sorption and biodegradation of organophosphorus pesticides during transport through Danube alluvial sediment. *J Environ Manag* 274, 111156. <https://doi.org/10.1016/j.jenvman.2020.111156>.
- Ore, O.T., Adeola, A.O., Bayode, A.A., Adepipe, D.T., Nomngongo, P.N., 2023. Organophosphate pesticide residues in environmental and biological matrices: occurrence, distribution and potential remedial approaches. *J Environ Chem Ecotoxicol* 5, 9–23. <https://doi.org/10.1016/j.enceco.2022.10.004>.
- Ugrina, M., Jurić, A., 2023. Current trends and future perspectives in the remediation of polluted water, soil and air - a review. *Processes* 11, 3270. <https://doi.org/10.3390/pr1123270>.
- Campos, P., Knicker, H., Miller, A.Z., Velasco-Molina, M., De la Rosa, J.M., 2021. Biochar ageing in polluted soils and trace elements immobilisation in a 2-year field experiment. *Environ Pollut* 290, 118025. <https://doi.org/10.1016/j.envpol.2021.118025>.
- Song, Q., Kong, F., Liu, B.F., Song, X., Ren, H.Y., 2024. Biochar-based composites for removing chlorinated organic pollutants: Applications, mechanisms, and perspectives. *Environ Sci Ecotechnol* 21, 100420. <https://doi.org/10.1016/j.ese.2024.100420>.
- Mukherjee, S., Sarkar, B., Aralappanavar, V.K., Mukhopadhyay, R., Basak, B.B., Srivastava, P., et al., 2022. Biochar-microorganism interactions for organic pollutant remediation: Challenges and perspectives. *Environ Pollut* 308, 119609. <https://doi.org/10.1016/j.envpol.2022.119609>.
- Qiu, M., Liu, L., Ling, Q., Cai, Y., Yu, S., Wang, S., et al., 2022. Biochar for the removal of contaminants from soil and water: a review. *Biochar* 4, 19. <https://doi.org/10.1007/s42773-022-00146-1>.
- Shaaban, M., Abid, M., 2021. Biochar as a sorbent for organic and inorganic pollutants. In: Núñez-Delgado, A. (Ed.), *Sorbents Materials for Controlling Environmental Pollution*. Elsevier, pp. 189–208. <https://doi.org/10.1016/B978-0-12-820042-1.00001-8>.
- Kookana, R.S., Sarmah, A.K., Van Zwieten, L., 2011. Biochar application to soil: agronomic and environmental benefits and unintended consequences. *Adv Agron* 2011 103–143. <https://doi.org/10.1016/B978-0-12-385538-1.00003-2>.
- Novak, J., Ro, K., Ok, Y.S., Sigua, G., Spokas, K., Uchimiya, S., et al., 2016. Biochars multifunctional role as a novel technology in the agricultural, environmental, and industrial sectors. *Chemosphere* 142, 1–3. <https://doi.org/10.1016/j.chemosphere.2015.06.066>.
- Bolan, N., Hoang, S.A., Beiyuan, J., Gupta, S., Hou, D., Karakoti, A., et al., 2022. Multifunctional applications of biochar beyond carbon storage. *Intern Mater Rev* 67, 150–200. <https://doi.org/10.1080/09506608.2021.1922047>.
- Bolan, N.S., Sarmah, A.K., Bordoloi, S., Van Zwieten, L., Solaiman, Z.M., Hailong, R., et al., 2023. Soil acidification and the liming potential of biochar. *Environ Pollut* 317, 120632. <https://doi.org/10.1016/j.envpol.2022.120632>.
- Ajeng, A.A., Abdullah, R., Ling, T.C., Ismail, S., Lau, B.F., Ong, H.C., et al., 2020. Bioformulation of biochar as a potential inoculant carrier for sustainable agriculture. *Environ Technol Inno* 20, 101168. <https://doi.org/10.1016/j.eti.2020.101168>.
- Wu, C., Zhi, D., Yao, B., Zhou, Y., Yang, Y., Zhou, Y., 2022. Immobilization of microbes on biochar for water and soil remediation: a review. *Environ Res* 212, 113226. <https://doi.org/10.1016/j.envres.2022.113226>.
- Mahmood Al-Nuaimy, N.M., Azizi, N., Nural, Y., Yabalak, E., 2024. Recent advances in environmental and agricultural applications of hydrochars: A review. *Environ Res* 250 (2024), 117923. <https://doi.org/10.1016/j.envres.2023.117923>.
- Kamalesh, S.R., Swaminaathan, P., Rangasamy, G., 2023. A comprehensive review on immobilized microbes - biochar and their environmental remediation: Mechanism, challenges and future perspectives. *Environ Res* 236, 116723. <https://doi.org/10.1016/j.envres.2023.116723>.
- Gong, Y.Z., Niu, Q.Y., Liu, Y.G., Dong, J., Xia, M.M., 2022. Development of multifarious carrier materials and impact conditions of immobilized microbial technology for environmental remediation: a review. *Environ Pollut* 22, 120232. <https://doi.org/10.1016/j.envpol.2022.120232>.
- Singh, B.K., Walker, A., 2006. Microbial degradation of organophosphorus compounds. *FEMS Microbiol Rev* 30 (3), 428–471. <https://doi.org/10.1111/j.1574-6976.2006.00018.x>.
- Robbins, M.P., Evansb, G., Valentinea, J., Donnisona, I.S., Allison, G.G., 2012. New opportunities for the exploitation of energy crops by thermochemical conversion in Northern Europe and the UK. *Prog Energ Combust* 38, 138–155. <https://doi.org/10.1016/j.peccs.2011.08.001>.
- Vučurović, D., 2015. Bioprocess model of ethanol production from sugar beet processing intermediates and byproducts, PhD Thesis, University of Novi Sad, Faculty of Technology, Novi Sad.
- Li, L., Long, A., Fossum, B., Kaiser, M., 2023. Effects of pyrolysis temperature and feedstock type on biochar characteristics pertinent to soil carbon and soil health: a meta-analysis. *Soil Use Manag* 39, 43–52. <https://doi.org/10.1111/sum.12848>.
- Mihajlović, M., Petrović, J., Maletić, S., Kragulj Isakovski, M., Stojanović, M., Lopičić, Z., et al., 2018. Hydrothermal carbonization of Miscanthus × giganteus: Structural and fuel properties of hydrochars and organic profile with the ecotoxicological assessment of the liquid phase. *Energy Convers Manag* 159, 254–263. <https://doi.org/10.1016/j.enconman.2018.01.003>.
- Kawnish, K., 2018. Chapter 4 - Thermochemical Conversion Processes for Waste Biorefinery in Waste Biorefinery. In: Bhaskar, T., Pandey, A., Venkata Mohan, S., Lee, D.J., Khanal, S.K. (Eds.), *Waste Biorefinery*. Elsevier, pp. 129–156. <https://doi.org/10.1016/C2016-0-02259-3>.
- Mumme, J., Eckervogt, L., Pielert, J., Diakité, M., Rupp, F., Kern, J., 2011. Hydrothermal carbonization of anaerobically digested maize silage. *Bioresour Technol* 102 (19), 9255–9260. <https://doi.org/10.1016/j.biortech.2011.06.099>.
- Gonçalves, C.N., Dalmolin, R.S.D., Dick, D.P., Knicker, H., Klamt, E., Kögel-Knabner, I., 2003. The effect of 10% HF treatment on the resolution of CPMA 13C NMR spectra and on the quality of organic matter in Ferralsols. *Geoderma* 116, 373–392. [https://doi.org/10.1016/S0016-7061\(03\)00119-8](https://doi.org/10.1016/S0016-7061(03)00119-8).
- Knicker, H., 2011. Solid state CPMA 13C and ¹⁵N NMR spectroscopy in organic geochemistry and how spin dynamics can either aggravate or improve spectra interpretation. *Org Geochem* 42, 867–890. <https://doi.org/10.1016/j.orggeochem.2011.06.019>.
- De la Rosa, J.M., Knicker, H., Lopez-Capel, E., Manning, D.A.C., Gonzalez-Perez, J. A., Gonzalez-Vila, F.J., 2008. Direct detection of black carbon in soils by Py-GC/MS, carbon-13 NMR spectroscopy and thermogravimetric techniques. *Soil Sci Soc Am J* 72, 258–267. <https://doi.org/10.2136/sssaj2007.0031>.
- Worch, E., 2004. Modelling the solute transport under nonequilibrium conditions on the basis of mass transfer equations. *J Contam Hydrol* 68, 97–120. [https://doi.org/10.1016/S0169-7722\(03\)00091-3](https://doi.org/10.1016/S0169-7722(03)00091-3).
- Johnson, J.L., Temple, K.L., 1964. Some Variables Affecting the Measurement of "Catalase Activity" in Soil. *Soil Sci Soc Am J* 28, 207–209. <https://doi.org/10.2136/sssaj1964.03615995002800020024x>.
- Roberge, M.R., 1978. Methodology of enzymes determination and extraction. In: Burns, R.G. (Ed.), *Soil Enzymes*. Academic Press, New York, pp. 341–373.
- Stepniewska, Z., Wolińska, A., Ziomek, J., 2009. Response of soil catalase activity to chromium contamination. *J Environ Sci* 21, 1142–1147. [https://doi.org/10.1016/S1001-0742\(08\)62394-3](https://doi.org/10.1016/S1001-0742(08)62394-3).
- Eivazi, F., Tabatabai, M.A., 1977. Phosphatases in soils. *Soil Biol Biochem* 9, 167–172. [https://doi.org/10.1016/0038-0717\(77\)90070-0](https://doi.org/10.1016/0038-0717(77)90070-0).
- Tabatabai, M.A., Bremner, J.M., 1969. Use of p-nitrophenyl phosphate for assay of soil phosphatase activity. *Soil Biol Biochem* 1, 301–307. [https://doi.org/10.1016/0038-0717\(69\)90012-1](https://doi.org/10.1016/0038-0717(69)90012-1).
- Thalman, A., 1968. Zur Methodik der Bestimmung der Dehydrogenase Aktivität in Boden Mittels Triphenyltetrazoliumchlorid (TTC). *Land Forsch* 21, 249–257.
- Dobler, R., Burrrf, P., Gruiz, K., et al., 2001. Variability in microbial populations in soil highly polluted with heavy metals on the basis of substrate utilization pattern Analysis. *J Soils Sediment* 1, 151–158. <https://doi.org/10.1007/BF02986478>.
- Garland, J.L., Mills, A.L., 1991. Classification and characterization of heterotrophic microbial communities on the basis of patterns of community-level sole-carbon-source utilization. *Appl Environ Microbiol* 57, 2351–2359. <https://doi.org/10.1128/aem.57.8.2351-2359.1991>.
- Weber, K.P., Legge, R.L., 2010. Community-level physiological profiling. *Methods Mol Biol* 599, 263–281. https://doi.org/10.1007/978-1-60761-439-5_16.

- [44] Metsalu, T., Vilo, J., 2015. ClustVis: a web tool for visualizing clustering of multivariate data using Principal Component Analysis and heatmap. *Nucleic Acids Res* 43, W566–W570. <https://doi.org/10.1093/nar/gkv468>.
- [45] Apprill, A., McNally, S., Parsons, R., Weber, L., 2015. Minor revision to V4 region SSU rRNA 806R gene primer greatly increases detection of SAR11 bacterioplankton. *Aquat Micro Ecol* 75, 129–137. <https://doi.org/10.3354/ame01753>.
- [46] Parada, A.E., Needham, D.M., Fuhrman, J.A., 2016. Every base matters: assessing small subunit <sc>rRNA</sc> primers for marine microbiomes with mock communities, time series and global field samples. *Environ Microbiol* 18, 1403–1414. <https://doi.org/10.1111/1462-2920.13023>.
- [47] Bolyen, E., Rideout, J.R., Dillon, M.R., et al., 2019. Reproducible, interactive, scalable and extensible microbiome data science using QIIME 2. *Nat Biotechnol* 37, 852–857. <https://doi.org/10.1038/s41587-019-0209-9>.
- [48] Estaki, M., Jiang, L., Bokulich, N.A., et al., 2020. QIIME 2 enables comprehensive end-to-end analysis of diverse microbiome data and comparative studies with publicly available data. *Curr Protoc Bioinform* 70. <https://doi.org/10.1002/cpbi.100>.
- [49] Hall, M., Beiko, R.G., 2018. 16S rRNA gene analysis with QIIME2. In: Beiko, R.G., Hsiao, W., Parkinson, J. (Eds.), *Microbiome Analysis. Methods in Molecular Biology*. vol 1849. Humana Press, New York, pp. 113–129. https://doi.org/10.1007/978-1-4939-8728-3_8.
- [50] Bokulich, N.A., Kaehler, B.D., Rideout, J.R., et al., 2018. Optimizing taxonomic classification of marker-gene amplicon sequences with QIIME 2's q2-feature-classifier plugin. *Microbiome* 6, 90. <https://doi.org/10.1186/s40168-018-0470-z>.
- [51] Quast, C., Pruesse, E., Yilmaz, P. et al., 2013. The SILVA ribosomal RNA gene database project: improved data processing and web-based tools. *Nucleic Acids Res* 41, D589–D596. <https://doi.org/10.1093/nar/gks1219>.
- [52] Fang, Y., Singh, B., Singh, B.P., Krull, E., 2014. Biochar carbon stability in four contrasting soils. *Eur J Soil Sci* 65, 60–71. <https://doi.org/10.1111/ejss.12094>.
- [53] Lehmann, J., Kleber, M., 2015. The contentious nature of soil organic matter. *Nature* 528, 60–68. <https://doi.org/10.1038/nature16069>.
- [54] Knicker, H., 2011. Soil organic N - An under-rated player for C sequestration in soils? *Soil Biol Biochem* 43, 1118–1129. <https://doi.org/10.1016/j.soilbio.2011.02.020>.
- [55] Paneque, M., De la Rosa, J.M., Kern, J., Reza, M.T., Knicker, H., 2017. Hydrothermal carbonization and pyrolysis of sewage sludges: What happen to carbon and nitrogen? *J Anal Appl Pyrol* 128, 314–323. <https://doi.org/10.1016/j.jaap.2017.09.019>.
- [56] Knicker, H., Velasco-Molina, M., Knicker, M., 2021. 2D Solid-State HETCOR ¹H–¹³C NMR experiments with variable cross polarization times as a tool for a better understanding of the chemistry of cellulose-based pyrochars—a tutorial. *Appl Sci* 11, 8569. <https://doi.org/10.3390/app11188569>.
- [57] Ukalska-Jaruga, A., Bejger, R., Smreczak, B., Podlasiński, M., 2023. Sorption of organic contaminants by stable organic matter fraction in soil. *Molecules* 28, 429. <https://doi.org/10.3390/molecules28010429>.
- [58] Apostolović, T., Trčković, J., Kragulj Isakovski, M., Jović, B., Maletić, S., Tubić, A., et al., 2020. Investigation of chlorinated phenols sorption mechanisms on different layers of the Danube alluvial sediment. *J Environ Sci* 224879416. <https://doi.org/10.1016/j.jes.2020.05.028>.
- [59] Zhou, X., Shi, L., Baghaee Moghaddam, T., Chen, M., Wu, S., Yuan, X., 2022. Adsorption mechanism of polycyclic aromatic hydrocarbons using wood waste-derived biochar. *J Hazard Mater* 425, 128003. <https://doi.org/10.1016/j.jhazmat.2021.128003>.
- [60] Du, Z., Huang, C., Meng, J., Yuan, Y., Yin, Z., Feng, L., et al., 2020. Sorption of aromatic organophosphate flame retardants on thermally and hydrothermally produced biochars. *Front Environ Sci Eng* 14, 43. <https://doi.org/10.1007/s11783-020-1220-6>.
- [61] Li, H.Z., Zhang, Y.N., Guo, J.Z., Lv, J.Q., Huan, W.W., Li, B., 2021. Preparation of hydrochar with high adsorption performance for methylene blue by co-hydrothermal carbonization of polyvinyl chloride and bamboo. *Bioresour Technol* 337, 125442. <https://doi.org/10.1016/j.biortech.2021.125442>.
- [62] Torsvik, V., Øvreås, L., 2002. Microbial diversity and function in soil: from genes to ecosystems. *Curr Opin Microbiol* 5, 240–245. <https://doi.org/10.1016/j.jenvp.2016.12.005>.
- [63] Kumar, S., Kaushik, G., Dar, M.A., et al., 2018. Microbial degradation of organophosphate pesticides: a review. *Pedosphere* 28, 190–208. [https://doi.org/10.1016/S1002-0160\(18\)60017-7](https://doi.org/10.1016/S1002-0160(18)60017-7).
- [64] Zhang, J., Shen, J.L., 2022. Effects of biochar on soil microbial diversity and community structure in clay soil. *Ann Microbiol* 72, 35. <https://doi.org/10.1186/s13213-022-01689-1>.
- [65] Bolan, S., Sharma, S., Mukherjee, S., Kumar, M., Rao, Ch.S., Nataraj, K.C., et al., 2024. Biochar modulating soil biological health: A review. *Sci Tot Environ* 914, 169585. <https://doi.org/10.1016/j.scitotenv.2023.169585>.
- [66] Jenkins, J.R., Viger, M., Arnold, E.C., Harris, Z.M., Ventura, M., Miglietta, F., et al., 2017. Biochar alters the soil microbiome and soil function: results of next-generation amplicon sequencing across Europe. *GCB Bioenergy* 9 (3), 591–612. <https://doi.org/10.1111/gcbb.12371>.
- [67] Singh, R.P., Yadav, R., Pandey, V., Singh, A., Singh, M., Shanker, K., et al., 2024. Effect of biochar on soil microbial community, dissipation and uptake of chlorpyrifos and atrazine. *Biochar* 6 (1), 17. <https://doi.org/10.1007/s42773-024-00306-5>.
- [68] Matchado, M.S., Rühlemann, M., Reitmeier, S., Kacprowski, T., Frost, F., Haller, D., et al., 2024. On the limits of 16S rRNA gene-based metagenome prediction and functional profiling. *Microb Genom* 10 (2), 001203. <https://doi.org/10.1099/mgen.0.001203>.
- [69] Nascimento, F.X., Hernández, A.G., Glick, B.R., Rossi, M.J., 2019. Plant growth-promoting activities and genomic analysis of the stress-resistant *Bacillus megaterium* STB1, a bacterium of agricultural and biotechnological interest. *Biotechnol Rep (Amst)* 4 (25), e00406. <https://doi.org/10.1016/j.btre.2019.e00406>.
- [70] Aswathi, A., Pandey, A., Sukumaran, R.K., 2019. Rapid degradation of the organophosphate pesticide - Chlorpyrifos by a novel strain of *Pseudomonas nitroreducens* AR-3. *Bioresour Technol*. 2019 Nov; 292,122025. <https://doi.org/10.1016/j.biortech.2019.122025>. Epub 2019 Aug 17. Erratum in: *Bioresour Technol*. 2020 Dec; 318,124093. <https://doi.org/10.1016/j.biortech.2020.124093>. PMID: 31466023.
- [71] Deng, S., Chen, Y., Wang, D., Shi, T., Wu, X., Ma, X., et al., 2015. Rapid biodegradation of organophosphorus pesticides by *Stenotrophomonas* sp. G1. *J Hazard Mater* 297, 17–24. <https://doi.org/10.1016/j.jhazmat.2015.04.052>.